Polymer 51 (2010) 3453–3461

Contents lists available at ScienceDirect

Polymer

journal homepage: www.elsevier.com/locate/polymer

# Elastomers with chain-end mussel-mimetic modification for nanocomposites: Strong modifications to reinforcement and viscoelastic properties

Xiao-Dong Pan*, Zengquan Qin, Yuan-Yong Yan, Pat Sadhukhan

*Bridgestone Americas Center for Research and Technology, 1200 Firestone Parkway, Akron, OH 44317-0001, United States*

ARTICLE INFO

*Article history:*
Received 8 March 2010
Received in revised form
7 May 2010
Accepted 15 May 2010
Available online 24 May 2010

*Keywords:*
Mussel-mimetic elastomers
Nanocomposite reinforcement
Payne effect

ABSTRACT

Depending on the nature and strength of interfacial interactions on the surface of nanoparticles, strong and unusual modifications to reinforcement and viscoelastic properties were observed for nanocomposites made of an elastomer with chain-end mussel-mimetic modification. Emulating 3,4-dihydroxyphenyl-L-alanine in marine mussel adhesive proteins, a styrene–butadiene random copolymer terminated with 3,4-dihydroxybenzaldehyde (DOBA) was prepared via living anionic polymerization. The nanocomposites were reinforced with either carbon black (hydrophobic), or amorphous precipitated silica (hydrophilic), or alumina-coated titanium oxide (hydrophilic). The DOBA end-group exhibits strong affinity to all three types of filler. In comparison to the corresponding nanocomposites made of a similar elastomer that bears no functional group, both the contrast in stress–strain relationship from tensile testing and the contrast in Payne effect from dynamic strain sweep testing display characters varying with the details of polymer–filler interactions currently not well understood.



## 1. Introduction

Pneumatic tires are indispensible for the motility of most motor vehicles. To a large extent, tread rubber compounds determine rolling loss (related to fuel consumption), wet skid resistance and durability of a tire. These sophisticated nanocomposites are typically vulcanized blend of a few elastomers reinforced with fine filler particles of carbon black and/or silica. Development of better tread compounds for balanced improvement of tire performance characters is no simple task as neither driving safety nor tread life (relating to generation of scrap tires) should be sacrificed for improvement of fuel economy [1]. In general, the rubber compounds need to be strongly reinforced, and their viscoelastic properties under dynamic deformation in both the zone of dynamic softening transition and rubbery state need to be properly tuned [2,3]. Due to the insufficient understanding on reinforcement mechanisms [4], rational material design remains a daunting challenge.

Starting from early 1990s [5], the combination of amorphous precipitated silica and silane coupling agents has become popular for reinforcement of tread compounds. When used in partial, or even in complete replacement of the conventional filler carbon black, significant reduction in rolling loss can be achieved. An unexpected gain in wet traction is also claimed along with acceptable wear resistance [6]. Beyond carbon black and silica as the primary fillers for reinforcement, other mineral particles such as aluminum hydroxide have also been examined for improvement of wet traction [7]. However, partially due to the lack of affinity between mineral particles and typical matrix elastomers, practical applications are hampered by the insufficient reinforcement level obtainable with most mineral particles.

The surface area for both carbon black and silica employed is of order of 100 $m^2/g$. For balanced reduction of rolling loss, chain-end modified elastomers have long been examined to promote strong interactions at the tremendous interface between filler particles and matrix elastomers [6,8,9]. A strong affinity between filler and matrix polymer can improve filler dispersion. An otherwise elastically ineffective dangling end of a polymer molecule chain can also become anchored to filler surface. Both factors contribute to strong and mostly desirable modifications to viscoelastic properties of rubber compounds. However, the identification of effective functional groups and the optimization of design is mostly a trial-and-error process. To address certain undesired consequences from usage of functionalized elastomers, from the perspective of functional group design, we have neither a definitive mechanistic understanding nor any guiding principle for design. In addition, the surface chemistry for the hydrophobic carbon black particles is radically different from that for the hydrophilic silica or other mineral particles [4]. Obviously a modified elastomer that exhibit strong affinity to all the different types of filler involved is very desirable.

* Corresponding author. Tel.: +1 330 379 7339; fax: +1 330 379 7530.
*E-mail address:* panxiaodong@bfusa.com (X.-D. Pan).

0032-3861/$ – see front matter © 2010 Elsevier Ltd. All rights reserved.
doi:10.1016/j.polymer.2010.05.031

Marine mussels adhere strongly to rock surface even in turbulent water. The mussel adhesive proteins, containing a high content of the amino acid 3,4-dihydroxy-L-phenylalanine (DOPA), stick to a wide variety of inorganic and organic surfaces [10]. The underlying mechanisms have been investigated extensively [11,12]. Extraordinarily strong yet reversible bonding between DOPA and titanium oxide surface was revealed from recent single-molecule measurements [13]. The phenomenon of mussel adhesion and the mechanistic understanding has stimulated the development of a number of innovative materials [14–18].

Mussel wet adhesion also inspires biomimetic consideration of improvement of wet traction. Thus we started with examining a styrene–butadiene rubber (SBR, random copolymer) that was terminated with 3,4-dihydroxybenzaldehyde (DOBA) for rubber compounding. As described below, it turns out that this DOBA end-group is the first simple (non-mosaic type) functional group discovered so far that exhibits strong affinity to all three types of fillers. Vulcanized compounds made of this modified SBR display a significant and balanced reduction in bulk hysteretic loss of relevance to tire rolling loss. Depending on the nature and strength of interactions between DOBA and the surface of different types of filler, the strong modifications to reinforcement and viscoelastic behavior of rubber compounds display interesting and new features.

In the following, unfilled and filled compounds made of this mussel-mimetic SBR (denoted as SBR-DOBA) are compared to corresponding compounds made of a reference SBR synthesized under very similar conditions but terminated with a proton (denoted as SBR-H). At similar volume fraction of filler, the filled compounds contain either a reinforcing grade of carbon black (C), or a reinforcing grade of precipitated silica ($SiO_2$), or a non-reinforcing grade of *alumina-coated* titanium oxide. Here pure titanium oxide without any surface coating is referred to as $TiO_2$ whereas the alumina-coated titanium oxide is represented with '$TiO_2$'.

## 2. Experimental section

### 2.1. Synthesis

#### 2.1.1. 3,4-Bis(tert-butyldimethylsiloxy)benzaldehyde (protected DOBA as the terminator)

Under nitrogen to a dry flask was charged 10.0 g 3,4-dihydroxybenzaldehyde, 16.1 g triethylamine, 0.35 g 4-(dimethylamino)pyridine, and 60 mL tetrahydrofuran (THF). Then a solution of 24.0 g tert-butyl(chloro)dimethylsilane in 60 mL methylene chloride was added in dropwise fashion. The reaction mixture was stirred for 1 h at room temperature (RT) prior to being poured into the mixture of 200 mL hexane and 100 mL saturated $NH_4Cl$ solution. The organic phase was then washed with three 100 mL portions of brine and dried with anhydrous $MgSO_4$.

After removal of the solvents, the residue was purified with a flash silica gel column, with hexane/ethyl acetate (95:5, v/v) as the eluent. After evaporation of the solvents, 25.5 g off-white solid was obtained (yield: 96%). $^1$H NMR (300 MHz, $CDCl_3$): $\delta$ 9.81 (s, 1H), 7.34–7.40 (m, 2H), 6.93 (d, $J = 8.5$ Hz, 1H), 0.995 (s, 9H), 0.992 (s, 9H), 0.247 (s, 6H), 0.227 (s, 6H). $^{13}$C NMR (300 MHz, $CDCl_3$): $\delta$ −4.31, −4.22, 18.26, 18.36, 25.71, 25.76, 120.44, 120.86, 125.39, 130.95, 147.72, 153.28, 190.53. Purity >99%.

#### 2.1.2. SBR-H

Under nitrogen to a dry 8-L reactor equipped with an agitator was charged 1393 g of hexane, 371 g of 33.0 wt% styrene in hexane and 2268 g of 21.6 wt% butadiene in hexane to give a 15.2 wt% monomer solution. It was followed with a charge of 3.19 mL of 1.6 M n-butyllithium solution in hexane and 1.13 mL of 1.6 M 2,2-bis(2′-tetrahydrofuryl)propane solution in hexane. The reactor jacket was then heated to 50 °C. After 75 min of polymerization run, the polymer cement was cooled to RT and dropped into isopropanol containing a small amount of 2,6-di-tert-butyl-4-methylphenol (BHT, as the antioxidant). The precipitated polymer was dried on a drum-drier at about 120 °C for a short duration.

#### 2.1.3. SBR-DOBA

The beginning steps were the same as those for SBR-H. After 75 min of polymerization run, 4.9 mL of 1.0 M 3,4-bis(tert-butyldimethylsiloxy)benzaldehyde solution in hexane was added to the reactor. The polymer cement was agitated for another 30 min at 50 °C, then cooled to RT, followed with addition of 12.0 mL of 1.0 M tetrabutylammonium fluoride solution in THF (containing ca. 5 wt% water). After the reactor was agitated at RT for 2 h, the polymer cement was coagulated with isopropanol containing a small amount of BHT. The precipitated polymer was dried in a vacuum oven heated to about 50 °C for 24 h. Drying with the drum-drier causes no noticeable difference (see the Supporting information for one example). The molecular structure for SBR-H and SBR-DOBA is schematically represented in Fig. 1.

#### 2.1.4. Verification of chain-end modifications

To demonstrate that the desired chain-end modifications were indeed achieved under the reaction conditions employed, two samples of low molecular weight polybutadiene rubber (BR) were

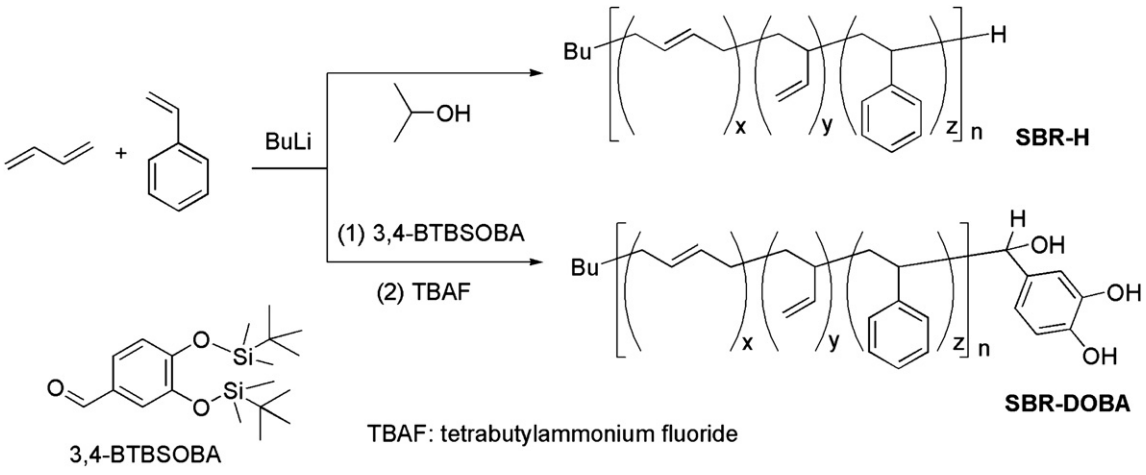


**Fig. 1.** Synthesis of SBR-H and SBR-DOBA.

synthesized via polymerization in a bottle. Under nitrogen, to a 150 mL bottle containing 50 g of 10.0 wt% butadiene in hexane was charged 1.04 mL of 1.6 M n-butyllithium. The bottle was agitated in a water-bath at 50 °C for 2.0 h. Then 1.67 mL of 1.0 M 3,4-bis(tert-butyldimethylsiloxy)benzaldehyde solution in hexane was added to the living polymer solution. The polymer cement was further agitated at 50 °C for 1 h, followed with addition of 1.0 mL of isopropanol. One half of the polymer solution was washed several times with isopropanol and the solvents were removed under reduced pressure, giving a viscous polymer. This BR sample bearing a chain-end protected DOBA group is denoted as BR-[DOBA]. The other half of the polymer solution was treated with TBAF (at [TBAF]/[$Li^+$] = 2.5) at RT for 3 h and then was worked up to give a viscous polymer of light brown color. This BR sample bearing a chain-end DOBA group is denoted as BR-DOBA. From GPC analysis of molecular weight distribution, $M_n$ is 4.7 and 5.7 kg/mol for BR-[DOBA] and BR-DOBA, respectively while $M_w/M_n$ is 1.15 and 1.35 for BR-[DOBA] and BR-DOBA, respectively. The $^1$H NMR spectra for the two BR samples are displayed in Fig. 2. Clearly, the protected DOBA groups are attached to chain ends for BR-[DOBA] and deprotection is accomplished for BR-DOBA.

### 2.2. Characteristics of SBR samples

Micro-structure of SBR molecules was obtained with $^1$H NMR. The results are listed in Table 1. Molecular weight distribution from GPC analysis is compared in Table 2. For the dried SBR-DOBA, 10.6% of the molecules become coupled. Such coupling does not exist for a dried SBR terminated with a protected DOBA group, prepared with a procedure similar to that for SBR-DOBA but without undergoing the deprotection step (see Table S-1 in the Supporting information). However, the coupling does not occur during the deprotection step. Instead, it arises from exposure to air, especially under heated condition. It is likely that a portion of polymer molecule chains becomes end-linked via di-DOBA coupling [19,20]. From DSC at the heating rate of 10 °C/min, the midpoint thermal glass transition temperature $T_g$ is −38.4 and −39.2 °C for SBR-H and SBR-DOBA, respectively.

For dried solid polymer samples, SBR-H is colorless while SBR-DOBA appears brown. For SBR terminated with a protected DOBA group (denoted as SBR-[DOBA]), the polymer remains colorless after drying. When stored indoor under ambient conditions or even at elevated humidity, SBR-DOBA remains stable.

**Table 1**
Micro-structure of SBR molecules.

| Polymer | Total styrene (%) | Block styrene[a] (%) | 1,2-Butadiene (%) | 1,4-Butadiene (%) |
|---|---|---|---|---|
| SBR-H | 21.0 | 1.4 | 38.8 | 40.2 |
| SBR-DOBA | 21.1 | 1.9 | 38.3 | 40.6 |

[a] Only micro-block containing 3–5 consecutive styrene units.

For practical purpose (storage and transportation), resistance to flow under self-weight (cold flow) is a desired character for an elastomer. Such cold flow resistance was examined with a cylindrical specimen molded at 100 °C under high pressure for 20 min. The mold cavity is 14.0 mm in diameter and 12.5 mm in height. After cooling down to RT, the cylindrical specimen was sandwiched between two parallel plates (with diameter much larger than 14.0 mm) at RT. Once a constant force of 49 (±0.5) N was applied at top, the specimen was squeezed without other lateral restriction. The variation of specimen height with time was recorded for 30 min and displayed in Fig. 3. Clearly the resistance to flow under an imposed force for SBR-DOBA is obviously better than that for SBR-H. The elevated coupling for SBR-DOBA only contributes a minor portion of this enhanced cold flow resistance (data not shown); the majority shall arise from the strong hydrogen bonding interactions among the chain-end DOBA groups.

### 2.3. Preparation of rubber compounds

A total of four different compounds were prepared with each SBR according to the formulations listed in Table 3. The specific fillers employed are carbon black of grade N339 according to the ASTM designation, silica of grade Hi-Sil® 190G from PPG Industries, and alumina-stabilized $TiO_2$ of grade CR-834 (bearing surface hydroxyl groups) from Tronox LLC. The three filled compounds are denoted as SBR/C, SBR/$SiO_2$ and SBR/'$TiO_2$', respectively. The density for C, $SiO_2$ and '$TiO_2$' is 1.8, 2.0 and 4.2 g/cm$^3$, respectively. Thus when the filler type is changed, the amount of filler is adjusted

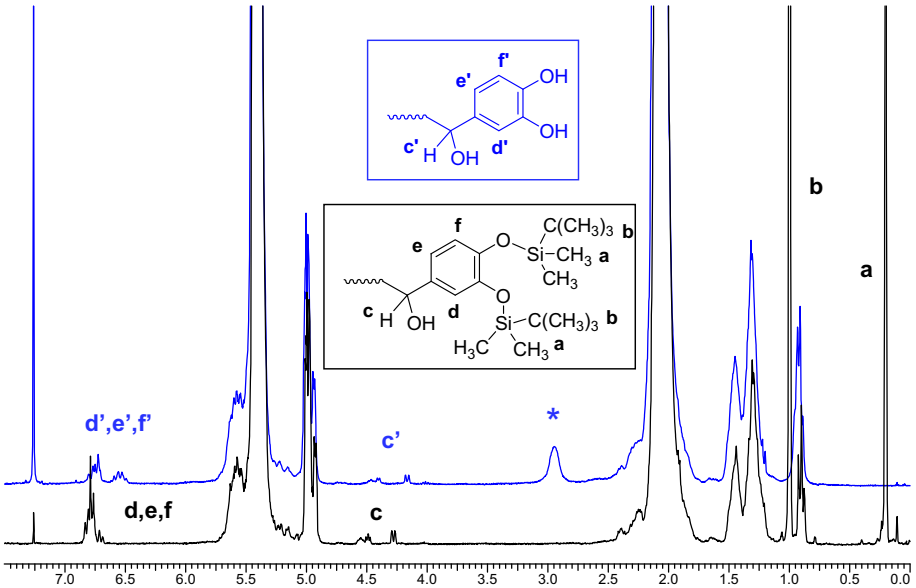


**Fig. 2.** $^1$H NMR spectra for the two end-modified polybutadiene samples. The black line depicts the spectrum for BR-[DOBA], which is terminated with a protected DOBA group. The blue line depicts the spectrum for BR-DOBA, which is terminated with a DOBA group (after deprotection).

**Table 2**
Molecular weight distribution of SBR samples.

| Polymer | $M_n$ (kg mol$^{-1}$) | $M_w/M_n$ | $M_{p1}$ (kg mol$^{-1}$) | $M_{p2}$ (kg mol$^{-1}$) | Amount of coupling (%) |
|---|---|---|---|---|---|
| SBR-H | 109.5 | 1.05 | 117 | 243.6 | 0.8 |
| SBR-DOBA | 120.3 | 1.12 | 123.2 | 258.9 | 10.6 |

for similar volume fraction of filler. A silane coupling agent was applied for the preparation of SBR/$SiO_2$ but not for SBR/'$TiO_2$'.

For these specific grades of filler particles utilized in this study, the typical primary particle size according to electron microscopy is between 26 and 30 nm for C, and is averaged at 17 and 170 nm for $SiO_2$ and '$TiO_2$', respectively. The nitrogen-adsorption surface area for C, $SiO_2$ and '$TiO_2$' is 96, 215 and 10.6 $m^2/g$, respectively. For both C and $SiO_2$, an individual filler entity actually consists of a number of primary particles fused together. In contrast, individual primary particles dominate for the case of '$TiO_2$'.

Following the common practice for achieving good mixing, compounding was performed with a laboratory internal mixer. The gum compounds (containing no filler) went through only two stages of mixing while all the filled compounds went through three stages of mixing (see Table S-3 for mixing temperature and other conditions in the Supporting information). The silane coupling agent Si 69 (from Evonik) was only applied to silica-filled compounds during the second stage of mixing. Testing samples were cured in appropriate molds heated to 165 °C under high pressure for a specified duration depending on the specific compound.

For the two gum compounds prior to crosslinking, possible change in polymer molecular weight distribution caused by the intensive mechanical mixing in the mixer was examined after each stage of mixing. Results from GPC analysis are listed in Table 4. The amount of coupling becomes slightly higher for SBR-DOBA.

### 2.4. Measurements of material properties

Tensile testing was performed with a model 4501 Instron Universal Testing Instrument. The specimen was in the shape of a micro-dumbbell. Its cross-section at center has the dimensions of 4.0 by 1.9 mm.

Measurements of viscoelasticity for the compounds were done with two Advanced Rheometric Expansion Systems from TA Instruments (one with high torque capability). The 'torsion rectangular' geometry was employed for dynamic temperature sweep tests. The dimensions for the die-cut specimens are about 47.0 by 12.7 by 1.9 mm.

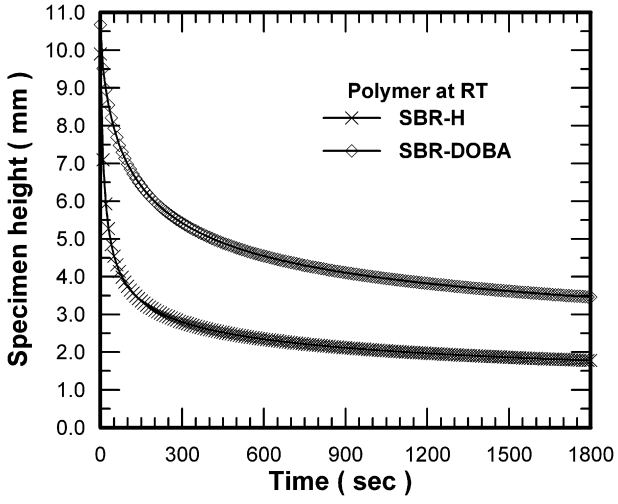


**Fig. 3.** Variation of specimen height with time under an imposed constant force of 49 N at RT (data recorded at the rate of 1 point every 10 s).

**Table 3**
Compounding formulas.

| (in phr)[a] | Compound designation | | | |
|---|---|---|---|---|
| | SBR | SBR/C | SBR/$SiO_2$ | SBR/'$TiO_2$' |
| SBR | 100.00 | 100.00 | 100.00 | 100.00 |
| Filler type | N/A | C | $SiO_2$ | '$TiO_2$' |
| Filler amount | 0.00 | 50.00 | 55.56 | 116.67 |
| Stearic acid | 2.00 | 2.00 | 2.00 | 2.00 |
| 6PPD[b] | 1.00 | 1.00 | 1.00 | 1.00 |
| Si 69[c] | 0.00 | 0.00 | 5.56 | 0.00 |
| Zinc oxide | 3.00 | 3.00 | 3.00 | 3.00 |
| DPG[d] | 0.50 | 0.50 | 0.50 | 0.50 |
| MBTS[d] | 1.00 | 1.00 | 1.00 | 1.00 |
| TBBS[d] | 0.00 | 0.00 | 1.00 | 1.00 |
| Sulfur | 1.30 | 1.30 | 1.15[e] | 1.30 |
| Total | 108.80 | 158.80 | 170.77 | 226.47 |

[a] The amount of each ingredient is specified in phr, or part per hundred rubber, by weight.
[b] The antidegradant 6PPD is N-(1,3-dimethylbutyl)-N′-phenyl-p-phenylenediamine.
[c] The bifunctional, sulfur-containing organosilane Si 69 is bis(triethoxysilylpropyl)polysulfide, only applied to silica-filled compounds during the second stage of mixing. Its sulfur content is 22.6% (by weight) [21]. With adjusted mixing conditions it can alternatively be added during the first stage of mixing.
[d] The vulcanization accelerators DPG, MBTS and TBBS represent diphenyl guanidine, dibenzothiazole disulfide and N-tert-butyl-2-benzothiazole sulfenamide, respectively [22].
[e] The amount of elemental sulfur is slightly reduced for SBR/$SiO_2$ as the bound sulfur in Si 69 also reacts with double bonds of polymer molecules during cure [5].

For the dynamic strain sweep tests, the parallel plate geometry was adopted. A cylindrical rubber specimen is about 7.8 mm in diameter and 5.8 mm in height. It was glued to the end plates with cyanoacrylate adhesive. Prior to acquiring the data presented here, all the specimens were exposed to similar large deformation. The option of 'one cycle correlate' was turned on during testing.

The extent of crosslinking can be compared with the equilibrium swelling test. The wet weight was acquired for specimens after over 72 h of immersion in toluene. The specimens were subsequently dried for 24 h in a vacuum oven heated to about 60 °C. The equilibrium swelling ratio (ESR) is defined here as the ratio of the volumes of the swollen and dried compounds.

Micro-scale filler dispersion was examined for all the filled compounds with a TEM (Philips CM12). Thin sections of a cross-linked compound of thickness between 70 and 100 nm were obtained via cryo-ultramicrotoming. They were deposited onto a copper mesh grid for imaging.

## 3. Results and discussion

The most direct embodiment of reinforcement effects from filler is the significantly enhanced tensile strength for filled compounds. At RT, uniaxial tensile testing was carried out at the strain rate of

**Table 4**
Mixing-induced change in polymer molecular weight distribution for the gum compounds (prior to crosslinking).

| Polymer | $M_n$ (kg mol$^{-1}$) | $M_w/M_n$ | $M_{p1}$ (kg mol$^{-1}$) | $M_{p2}$ (kg mol$^{-1}$) | Amount of coupling (%) |
|---|---|---|---|---|---|
| *After first stage of mixing* | | | | | |
| SBR-H | 104.1 | 1.03 | 107.8 | 215.3 | 1.2 |
| SBR-DOBA | 116.7 | 1.12 | 111.4 | 221.2 | 15.4 |
| *After final stage of mixing (with milder intensity)* | | | | | |
| SBR-H | 104.2 | 1.03 | 107.9 | 216.2 | 1.2 |
| SBR-DOBA | 117.1 | 1.13 | 111.6 | 221.4 | 15.4 |

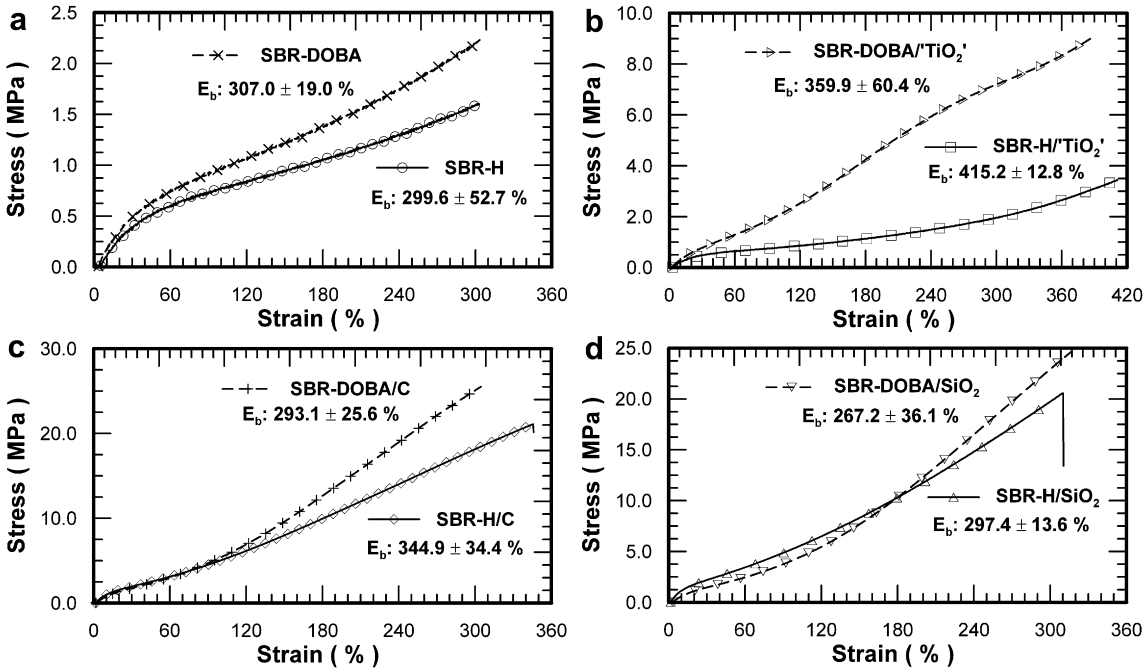


**Fig. 4.** Representative (engineering) stress–strain relationship from uniaxial tensile testing at RT. Average value of elongation at break ($E_b$) as obtained from testing of three or four specimens is marked for each compound. (a) For the gum compounds. (b) For the compounds filled with '$TiO_2$'. (c) For the compounds filled with C. (d) For the compounds filled with $SiO_2$.

0.223 $s^{-1}$. Engineering stress is plotted against strain in Fig. 4 for all the compounds. For the two gum compounds, at the same strain, the stress required to deform SBR-DOBA is larger than that for SBR-H. Value of ESR is 6.81 (±0.015) and 6.04 (±0.015) for SBR-H and SBR-DOBA, respectively. For SBR-DOBA, in addition to crosslinking formed by atomic bridges of sulfur, a portion of the polymer molecules exists in coupled state possibly formed via end-linking (see Tables 2 and 4). Such additional coupling likely contributes to the higher stress required for deformation and the lower ESR value for SBR-DOBA.

Due to the large particle size, and especially the absence of specific affinity between SBR-H and '$TiO_2$', SBR-H/'$TiO_2$' is not significantly reinforced. In contrast, the reinforcement effect becomes much enhanced when the matrix polymer is SBR-DOBA. At all strain level prior to break, the stress required to deform SBR-DOBA/'$TiO_2$' is larger than that for SBR-H/'$TiO_2$'.

Comparing the tensile behavior for SBR-H/C and SBR-H/$SiO_2$ to that for the gum compounds, even the non-functionalized polymer SBR-H becomes tremendously reinforced with fine particles of either $SiO_2$ (along with a coupling agent) or C. When the functionalized SBR-DOBA is filled with either C or $SiO_2$, the stress necessary to deform either SBR-DOBA/C or SBR-DOBA/$SiO_2$ to sufficiently large strain is still larger than that for the corresponding compound made of SBR-H. However, at strain less than about 75%, the stress required to deform SBR-DOBA/C is only slightly lower than that for SBR-H/C. At strain less than about 180%, the stress required to deform SBR-DOBA/$SiO_2$ is more obviously lower than that for SBR-H/$SiO_2$.

Discrete values of stress at different levels of deformation are listed in Table 5 for all the compounds. Overall for filled compounds of SBR-DOBA, the stronger polymer–filler interactions typically result in a shorter elongation at break. As exemplified in Table 6, when processing oil is employed for compounding, the elongation at break can be significantly increased.

Via a variety of different interaction mechanisms, various parts of a polymer molecule can become attached to the surface of a single or even multiple filler particles. In this way, filler particles effectively act as extra points of crosslink in addition to those due to sulfur. Thus for filled compounds, it is reasonable to expect that the ESR value approximately decreases with increasing strength of polymer–filler interactions. Consistent with such expectation, the ESR value decreases from 5.39 (±0.010) for SBR-H/'$TiO_2$' to 3.87 for SBR-DOBA/'$TiO_2$', and from 3.83 for SBR-H/C to 3.71 for SBR-DOBA/C.

**Table 5**
Values of stress at various strains.[a]

| Cross-linked compounds | Engineering stress at different strain (MPa) | | | | | Strain (%) |
|---|---|---|---|---|---|---|
| | At 50% | At 100% | At 200% | At 300%[b] | At break | At break |
| SBR-H | 0.57 ± 0.05 | 0.77 ± 0.04 | 1.14 ± 0.04 | (1.62 ± 0.06) | 1.6 ± 0.3 | 299.6 ± 52.7 |
| SBR-DOBA | 0.66 ± 0.01 | 0.97 ± 0.01 | 1.49 ± 0.01 | (2.19 ± 0.02) | 2.3 ± 0.2 | 307.0 ± 19.0 |
| SBR-H/C | 2.73 ± 0.03 | 5.07 ± 0.07 | 11.30 ± 0.08 | (18.04 ± 0.14) | 20.8 ± 2.0 | 344.9 ± 34.4 |
| SBR-DOBA/C | 2.50 ± 0.05 | 5.25 ± 0.11 | 14.56 ± 0.18 | (25.14 ± 0.07) | 24.3 ± 2.6 | 293.1 ± 25.6 |
| SBR-H/$SiO_2$ | 3.00 ± 0.05 | 5.37 ± 0.08 | 11.72 ± 0.19 | (19.56 ± 0.20) | 19.5 ± 1.0 | 297.4 ± 13.6 |
| SBR-DOBA/$SiO_2$ | 2.02 ± 0.10 | 4.04 ± 0.22 | 11.93 ± 0.28 | (22.94 ± NA) | 19.2 ± 4.0 | 267.2 ± 36.1 |
| SBR-H/'$TiO_2$' | 0.59 ± 0.02 | 0.78 ± 0.02 | 1.23 ± 0.03 | 1.92 ± 0.06 | 3.4 ± 0.1 | 415.2 ± 12.8 |
| SBR-DOBA/'$TiO_2$' | 1.11 ± 0.04 | 2.03 ± 0.04 | 4.78 ± 0.10 | (7.11 ± 0.14) | 8.4 ± 1.2 | 359.9 ± 60.4 |

[a] Expressed as average ± standard deviation. Three specimens were tested for SBR-H/'$TiO_2$' and SBR-DOBA/'$TiO_2$' while four specimens were tested for all other compounds.
[b] Values listed in () indicate that not all the specimens tested withstood deformation up to the strain of 300%.

**Table 6**
Values of stress at various strains for compounds containing processing oil.[a, b]

| Cross-linked compounds | Engineering stress at different strain (MPa) | | | | | Strain (%) |
|---|---|---|---|---|---|---|
| | At 50% | At 100% | At 200% | At 300% | At break | At break |
| SBR-H/C | 1.73 ± 0.03 | 3.13 ± 0.06 | 7.03 ± 0.11 | 11.66 ± 0.09 | 18.5 ± 1.0 | 446.0 ± 23.2 |
| SBR-DOBA/C | 1.72 ± 0.04 | 3.51 ± 0.09 | 9.99 ± 0.19 | 18.09 ± 0.18 | 24.2 ± 1.2 | 380.7 ± 15.1 |
| SBR-H/$SiO_2$ | 2.22 ± 0.06 | 4.01 ± 0.10 | 8.68 ± 0.21 | 14.50 ± 0.27 | 18.9 ± 1.0 | 367.3 ± 16.8 |
| SBR-DOBA/$SiO_2$ | 1.58 ± 0.09 | 3.15 ± 0.21 | 9.21 ± 0.29 | 18.03 ± 0.10 | 21.1 ± 1.9 | 333.9 ± 20.5 |

[a] The formulations were the same as those displayed in Table 3 except that 10.0 phr of a naphthenic-based processing oil was added during the first stage of mixing.
[b] Four specimens were tested for each compound.

To the contrary, the ESR value increases from 3.50 (±0.017) for SBR-H/$SiO_2$ to 3.62 (±0.004) for SBR-DOBA/$SiO_2$. For SBR-H/$SiO_2$, the silanol groups on silica surface react only with molecules of the silane coupling agent that also react with the double bonds along polymer chains [5]. There exists no specific affinity between chain ends of SBR-H and silica surface. For the case of SBR-DOBA/$SiO_2$, chain-end DOBA groups can become attached to silica surface, thus reducing the number of silanol groups available for reaction with silane. Measured with ESR, the higher value for SBR-DOBA/$SiO_2$ seems to suggest that the DOBA/$SiO_2$ interaction is weaker than the binding established via silane coupling reaction. However, from tensile testing displayed in Fig. 2(d), at large enough strain, the stress required to deform SBR-DOBA/$SiO_2$ is still higher than that for SBR-H/$SiO_2$. Furthermore, for silica-filled compounds prepared with SBR bearing other types of chain-end functional groups that do form covalent bonding with silica surface, value of ESR can be less than that for SBR-H/$SiO_2$ while the contrast with SBR-H/$SiO_2$ in stress–strain behavior from tensile testing still displays similar qualitative features.

Cross-linked rubber compounds are imperfectly elastic solids. Their viscoelastic behavior is frequently described in terms of storage modulus $G'$ and loss modulus $G''$. They are obtained from the analysis of stress response under an imposed sinusoidal strain $\gamma = \gamma_0 \sin(2\pi ft)$, here $\gamma_0$ and $f$ indicates strain amplitude and oscillation frequency, respectively. Loss tangent $\tan\delta$ $(=G''/G')$ describes the ratio of energy dissipated to the energy reversibly exchanged in dynamic loading. Rubber viscoelasticity typically varies with temperature $T$, $\gamma_0$ and $f$. The pronounced nonlinear dependency of $G'$ and $G''$ on $\gamma_0$ for filled rubber compounds is widely known as the Payne effect [2,23]. The exact mechanisms underlying such prominent nonlinearity are not yet completely resolved. Most people adopt the concept of filler networking originally proposed by Payne [23].

For development of better tread rubber compounds, it has long become an established practice in tire industry to correlate certain tire performance characters with hysteretic loss property of rubber compounds as represented by tan $\delta$ [2]. At typical driving speeds, energy loss during rolling of a whole tire involves material deformation with $f$ between $10^1$ and $10^2$ Hz and $T$ between 50 and 80 °C [2]. For a tire sliding over road surface bearing multi-scale asperities, wet skid resistance arises from energy dissipation during dynamic deformation of tread compounds with $f$ between $10^3$ and $10^7$ Hz [2].

Strong polymer–filler interactions cause dramatic change in bulk hysteretic loss for filled compounds. This is clearly revealed from the variation of tan $\delta$ with $T$ as displayed in Fig. 5 for all the compounds. The testing was performed at 10 Hz under small deformation: with $\gamma_0$ at 0.20% for $T \leq -5$ °C and $\gamma_0$ at 2.0% for $T \geq 0$ °C. Within the zone of softening transition from glass to rubberlike state where $G'$ decreases rapidly with increasing $T$, a distinct peak in tan $\delta$ appears at about −22 °C. The peak height and shape are very similar to each other for the two gum compounds. In comparison, the filled compounds display reduced peak height and increased peak width at half height. Such characters are affected by filler amount, filler particle size distribution and filler dispersion. Regardless of the specific type of filler, in

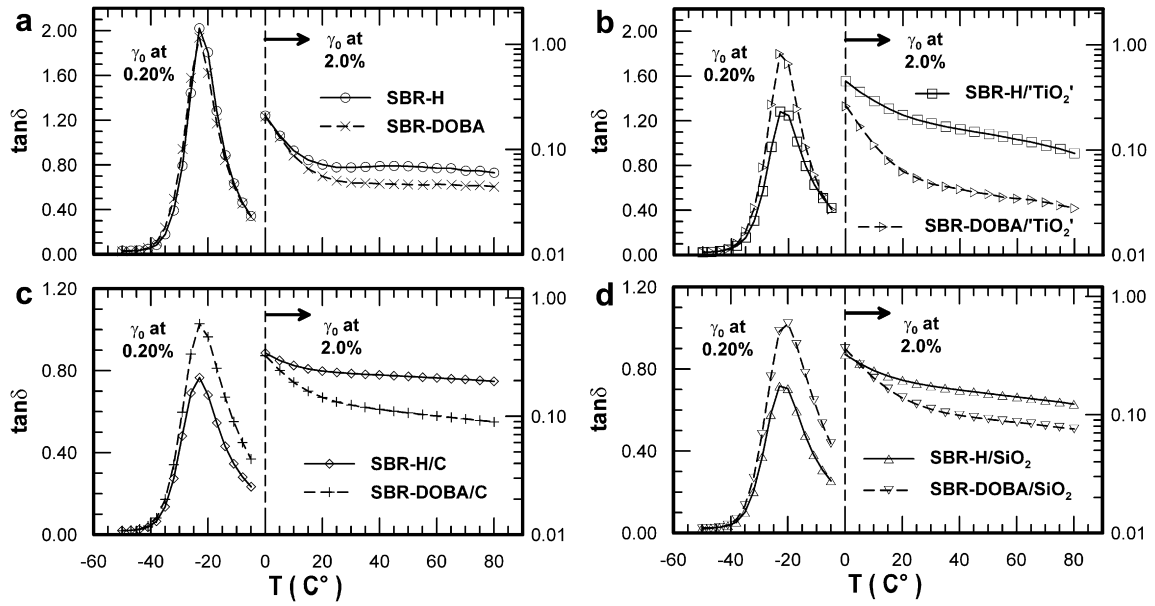


**Fig. 5.** Variation of tan $\delta$ with temperature from dynamic temperature sweep testing at 10.0 Hz. For $T < 0$ °C, tan $\delta$ is scaled according to the left vertical axis while for $T \geq 0$ °C, tan $\delta$ is scaled according to the right vertical axis.

comparison to a filled compound prepared with SBR-H, the corresponding filled compound made of SBR-DOBA displays a significantly increased peak height. This arises primarily from improved filler dispersion due to the strong affinity between DOBA and filler surface. At this peak in tan $\delta$ (with $\gamma_0$ at 0.20%), the better filler dispersion leads to more obvious reduction in $G'$ than that for $G''$. As shown in Fig. 6, TEM images of micro-scale filler dispersion confirm that in comparison to a filled compound made of SBR-H, filler particle distribution becomes obviously more uniform in the corresponding filled compound made of SBR-DOBA.

At high $T$ of relevance to tire rolling loss, tan $\delta$ is always lower for the compounds made of SBR-DOBA. The improved filler dispersion due to the strong affinity between DOBA and filler surface diminishes interactions among filler particles. The breakdown and reformation of a weakened filler network generates less hysteretic loss at large $\gamma_0$. Free dangling ends of polymer molecules are elastically ineffective and dissipate energy. The DOBA end-group anchors one end of a polymer molecule chain to the filler surface thus reduces tan $\delta$ further. Here SBR-DOBA/'$TiO_2$' displays the lowest tan $\delta$, even less than that for the gum compound SBR-DOBA. Overall as expected, tan $\delta$ for silica-filled compounds is lower than that for the corresponding carbon black-filled compounds.

Empirically, from the perspective of energy dissipation via bulk hysteretic loss, the combination of a higher tan $\delta$ at low $T$ and a lower tan $\delta$ at high $T$ suggests a tread compound with low rolling loss and good wet skid resistance [2]. However, improvement of wet traction due to direct wet adhesive interactions between DOBA groups and road surface was never detected even for the gum compound SBR-DOBA, even though this was one of the original inspirations that motivated this study. One possible reason is that under the conditions employed for testing of wet skid resistance (sliding speed at ~1 m/s), no effective contact was established between DOBA groups (if ever present on rubber surface) and the rough road surface.

To further corroborate the unique reactivity of the DOBA group, adopting the same formulations shown in Table 3, filled compounds were also prepared with SBR-[DOBA] that is terminated with a protected DOBA group. From dynamic temperature sweep testing, variation of tan $\delta$ with $T$ for such compounds is almost identical to that for the corresponding filled compounds made of SBR-H (see Fig. S-1 in the Supporting information). Thus a protected DOBA group does not exhibit strong affinity to the surface of any filler examined in this study.

The above features revealed from dynamic temperature sweep testing are further examined with dynamic strain sweep testing (Fig. 7). Rolling loss of rubber compounds is typically compared with tan $\delta$ measured at 60 °C and 10 Hz. As displayed in Fig. 7(a), between $\gamma_0$ of 1% and $\gamma_0$ of 25%, value of tan $\delta$ for a compound of SBR-DOBA is significantly lower than that for the corresponding compound made of SBR-H. At $\gamma_0$ of 9.95%, value of tan $\delta$ is 0.101, 0.208 ($\pm$0.006), 0.186 and 0.101 for SBR-H, SBR-H/C, SBR-H/$SiO_2$ and SBR-H/'$TiO_2$', respectively. It becomes 0.0647, 0.0968, 0.0840 and 0.0428 for SBR-DOBA, SBR-DOBA/C, SBR-DOBA/$SiO_2$ and SBR-DOBA/'$TiO_2$', respectively. Thus for a filled compound made of SBR-DOBA, tan $\delta$ at $\gamma_0$ of 9.95% is less than half of that for the corresponding compound made of SBR-H. With the non-reinforcing '$TiO_2$', tan $\delta$ for SBR-H/'$TiO_2$' is very close to that for the gum compound SBR-H. In comparison to SBR-H/'$TiO_2$', SBR-DOBA/'$TiO_2$' is significantly more reinforced, and tan $\delta$ for SBR-DOBA/'$SiO_2$' is even lower than that for the gum compound SBR-DOBA.

As described previously, from temperature sweep testing at small $\gamma_0$, the peak in tan $\delta$ for the filled compounds prepared with SBR-DOBA is obviously higher than that for the corresponding compounds of SBR-H. At 1.0 Hz (data not shown), the temperature where the peak in tan $\delta$ appears, $T_{\text{Peak tan }\delta}$, is between −28.4 and −26.4 °C for all the compounds. At $T$ slightly higher than $T_{\text{Peak tan }\delta}$, tan $\delta$ increases with decreasing $T$.

At 1.0 Hz and about −23 °C, variation of tan $\delta$ with $\gamma_0$ is plotted in Fig. 7(b) for all the compounds. For $\gamma_0 < 0.5\%$, the qualitative ranking in tan $\delta$ among the compounds is consistent with that at $T$ slightly higher than $T_{\text{Peak tan }\delta}$ shown in Fig. 5. Here tan $\delta$ for a filled compound of SBR-DOBA is higher than the corresponding filled

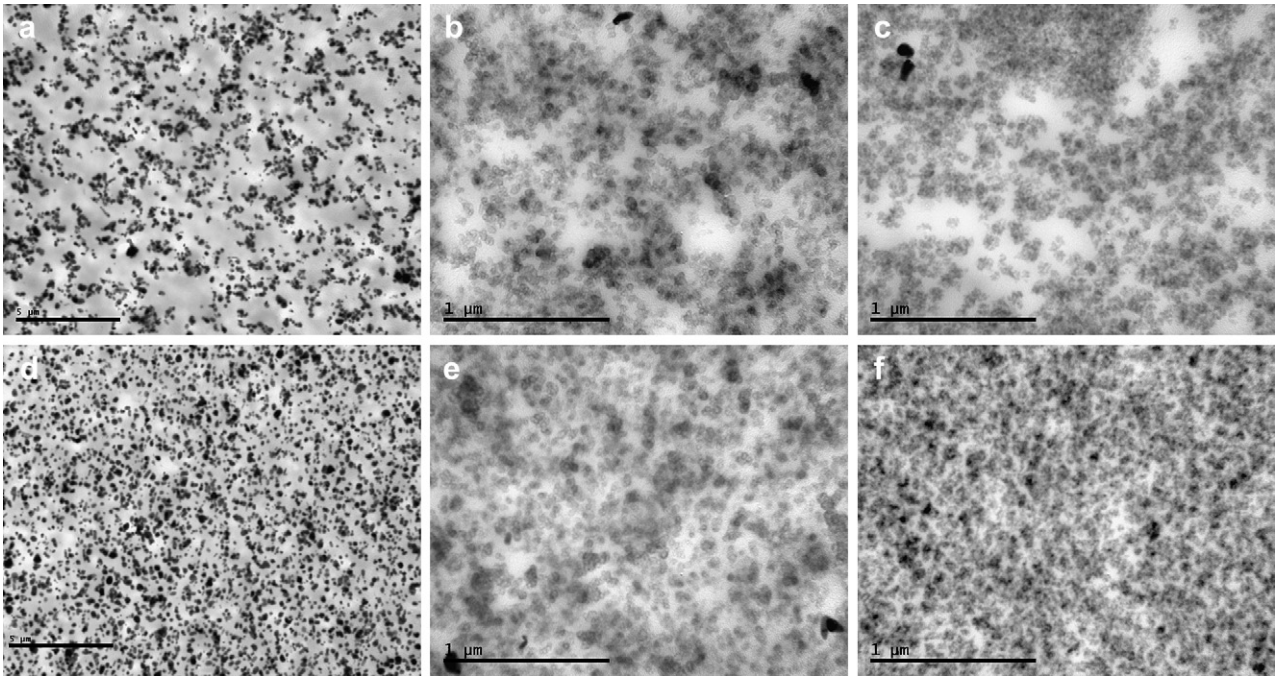


**Fig. 6.** TEM images revealing micro-scale filler dispersion for (a) SBR-H/'$TiO_2$', (b) SBR-H/C, (c) SBR-H/$SiO_2$, (d) SBR-DOBA/'$TiO_2$', (e) SBR-DOBA/C, and (f) SBR-DOBA/$SiO_2$. The scaling bar corresponds to 5 μm in (a) and (d), or 1 μm in (b), (c), (e) and (f).

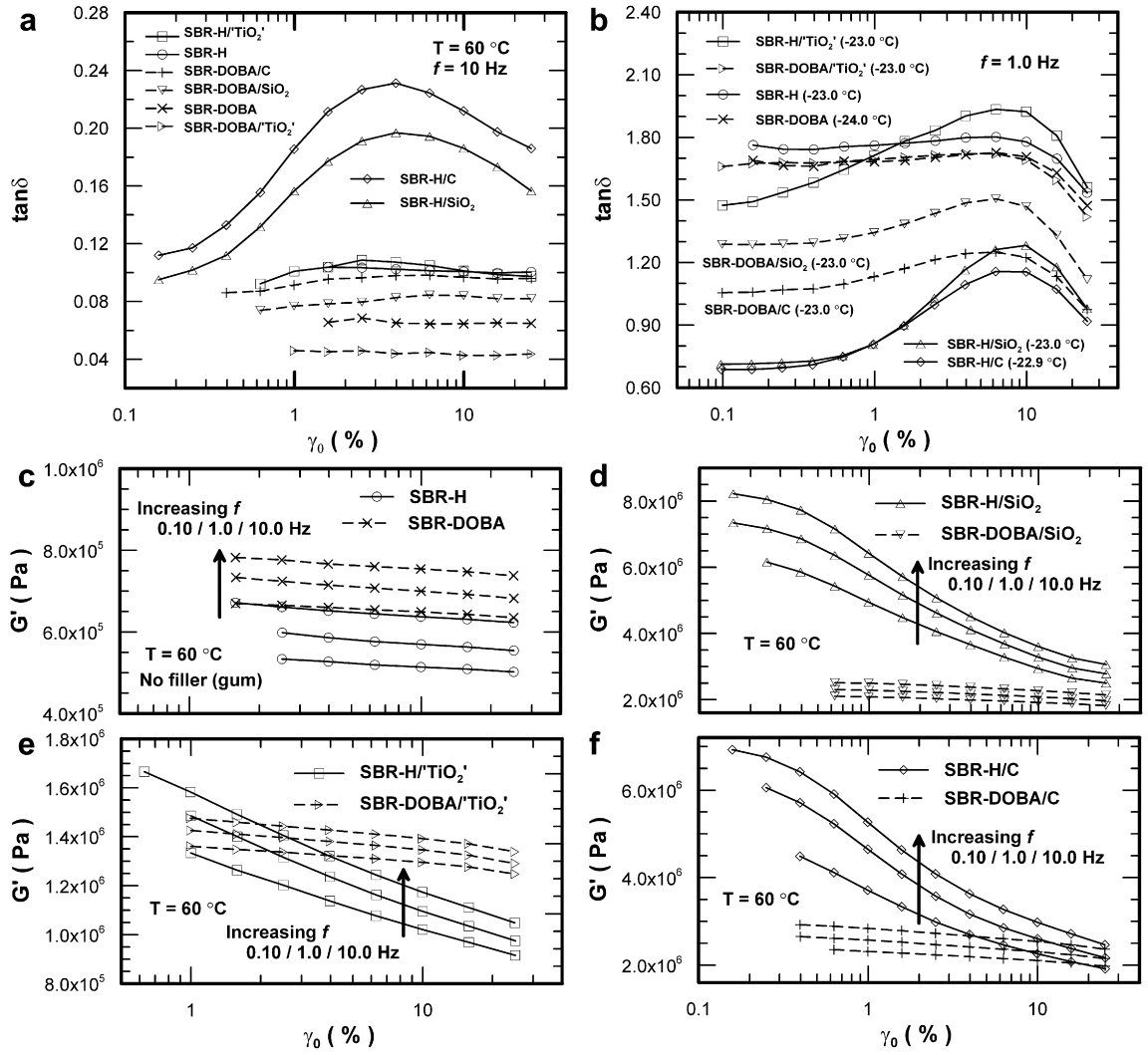


**Fig. 7.** Variation of tan $\delta$ or $G'$ with $\gamma_0$ from dynamic strain sweep testing under different conditions. (a) For all the compounds at 60 °C and 10 Hz; (b) For all the compounds at about −23 °C and 1.0 Hz; (c–f) Variation of $G'$ with $\gamma_0$ for all the compounds at 60 °C. The arrows appeared in (c–f) indicate the direction of increasing frequency.

compound made of SBR-H. However, for $\gamma_0$ between 2% and 25%, tan $\delta$ for SBR-H/'$TiO_2$' becomes higher than tan $\delta$ for SBR-DOBA/'$TiO_2$' due to the significantly weakened filler–filler interactions in SBR-DOBA/'$TiO_2$'.

For better vehicle/tire handling characteristics such as quick steering response, a stiffer compound can be desirable. Variation of $G'$ with $\gamma_0$ at 60 °C is examined for all the compounds at 0.10, 1.0 and 10.0 Hz. For the full range of $\gamma_0$ examined, $G'$ increases with $f$. Due to the higher degree of crosslinking for the gum compound SBR-DOBA, its $G'$ is always higher than $G'$ for the corresponding gum compound SBR-H (Fig. 7(c)). However, the situation becomes reversed for the case of silica-filled compounds (Fig. 7(d)). As typically observed for compounds prepared with other types of chain-end modified elastomers (filled with either C or $SiO_2$), along with a significant reduction in tan $\delta$, $G'$ for SBR-DOBA/$SiO_2$ appears lower than $G'$ for SBR-H/$SiO_2$ throughout the range of $\gamma_0$ examined. This can be undesirable for tire handling response. For reinforced compounds made of different functionalized elastomers, at 60 °C and at large $\gamma_0$, a reduction in $G'$ about proportional to the decrease in tan $\delta$ frequently emerges. There currently exists no guiding principle for rational design of functional group to counter such undesirable trend.

Here comes a surprise with SBR-DOBA/'$TiO_2$' (Fig. 7(e)). At sufficiently low $\gamma_0$, $G'$ is higher for SBR-H/'$TiO_2$'. However, at higher $\gamma_0$ of relevance to tire performance, SBR-DOBA/'$TiO_2$' exhibits a higher $G'$. The strain at which the crossover in $G'$ occurs increases with increasing $f$. Compounds reinforced with C also display qualitatively similar features (Fig. 7(f)), but $\gamma_0$ at the crossover in $G'$ is about one order of magnitude higher than that for the compounds filled with '$TiO_2$'. These constitute the first observations of such crossover in $G'$ for reinforced compounds prepared with chain-end modified elastomers. Overall, from the variation of either $G'$ or tan $\delta$ with $\gamma_0$, the nonlinearity in viscoelasticity is much reduced for filled compounds of SBR-DOBA.

Thus far we have seen that between a filled compound of SBR-H and the corresponding filled compound of SBR-DOBA, both the contrast in stress–strain relationship from tensile testing and the contrast in variation of $G'$ with $\gamma_0$ from strain sweep testing varies with the type of filler. This shall originate mainly from the different nature and intensity of interactions between DOBA and the surface of different types of filler, which remains to be clarified. In literature the force-distance relationship for DOPA interacting with a surface has only been reported for a few cases. The interaction between DOPA and $TiO_2$ surface is attributed to a strong and reversible

coordination bonding [13] (not directly applicable here due to the alumina surface coating) while the adhesion between DOPA and the more inert mica surface is attributed to weak physical interactions such as hydrogen bonding [24].

## 4. Concluding remarks

Emulating the celebrated phenomenon of mussel wet adhesion, we synthesized an SBR terminated with a DOBA group. This new functional group for modification of polymer–filler interactions exhibits strong affinity to both hydrophobic carbon black and hydrophilic inorganic oxides. As a consequence, profound modifications to reinforcement and viscoelastic properties are observed for nanocomposites prepared with this SBR-DOBA. Depending on the nature and strength of interfacial interactions (not-well characterized so far), modifications to viscoelastic behavior display interesting and new characters never reported before. Overall, this mussel-mimetic SBR-DOBA demonstrates great promise for balanced improvement of tire performances.

Beyond this chain-end catecholic group, the whole class of hydroxyphenyl groups (including monohydroxy-, dihydroxy- and trihydroxy-phenyl) can be exploited for beneficial modification of polymer–filler interactions. This new class of modified elastomers exhibits many interesting characters, such as improved resistance to cold flow for SBR-DOBA arising from the strong hydrogen bonding interactions among chain-end DOBA groups. Furthermore, such functional groups can be incorporated onto polymer molecule chains with much flexibility: at initiation, at termination and/or along the backbone. Numerous possibilities for design of modification exist for tuning polymer–filler interactions. Clearly exciting opportunities lie ahead for further revelation of relationship between polymer–filler interactions and reinforcement of rubber compounds.

## Acknowledgement

The authors wish to thank Bridgestone Americas Holding, Inc. for permission to publish this work. Special thanks go to Mr. Edward D. Kelley, Mr. Dennis R. Brumbaugh and Dr. Michael W. Hayes for their testing support.

## Appendix. Supporting information

Tables giving molecular weight distribution and micro-structure information for three additional SBR samples including one terminated with a protected DOBA group; table revealing detailed mixing conditions for the eight compounds discussed, and figure showing the absence of affinity between a protected DOBA group and filler surface. Supplementary data associated with this article can be found in the online version at doi:10.1016/j.polymer.2010.05.031.

## References

[1] Committee for the National Tire Efficiency Study, Transportation Research Board. Tires and passenger vehicle fuel economy: informing consumers, improving performance. Washington DC: National Research Council of the National Academies; 2006.
[2] Wang MJ. Rubber Chem Technol 1998;71:520–89.
[3] Grosch KA. Rubber Chem Technol 1996;69:495–568.
[4] Donnet JB. Rubber Chem Technol 1998;71:323–41.
[5] Wolff S, Gorl U, Wang MJ, Wolff W. Eur Rubber J 1994;176:16–9.
[6] Fujimaki T, Morita K. Int Polym Sci Technol 1999;26:26–34.
[7] Mouri H, Akutagawa K. Rubber Chem Technol 1999;72:960–8.
[8] Schuring DJ, Futamura S. Rubber Chem Technol 1990;63:315–67.
[9] Quirk RP, Yin J, Guo SH, Hu XW, Summers GJ, Kim J, et al. Rubber Chem Technol 1991;64:648–60.
[10] Crisp DJ, Walker G, Young GA, Yule AB. J Colloid Interface Sci 1985;104:40–50.
[11] Waite JH, Tanzer ML. Science 1981;212:1038–40.
[12] Yu M, Hwang J, Deming TJ. J Am Chem Soc 1999;121:5825–6.
[13] Lee H, Scherer NF, Messersmith PB. Proc Natl Acad Sci USA 2006;103:12999–3003.
[14] Li K, Liu Y. U.S. Patent 7,060,798; June 13, 2006.
[15] Podsiadlo P, Liu Z, Paterson D, Messersmith PB, Kotov NA. Adv Mater 2007;19:949–55.
[16] Lee H, Dellatore SM, Miller WM, Messersmith PB. Science 2007;318:426–30.
[17] Westwood G, Horton TN, Wilker JJ. Macromolecules 2007;40:3960–4.
[18] Hamming LM, Fan XW, Messersmith PB, Brinson LC. Compos Sci Technol 2008;68:2042–8.
[19] McDowell LM, Burzio LA, Waite JH, Schaefer J. J Biol Chem 1999;274:20293–5.
[20] Burzio LA, Waite JH. Biochemistry 2000;39:11147–53.
[21] Organosilane product information Si 69 (PI320) from Evonik.
[22] Coran AY. Vulcanization. In: Mark JE, Erman B, Eirich FR, editors. Science and technology of rubber. 2nd ed. San Diego: Academic Press; 1994. p. 339–85.
[23] Payne AR, Whittaker RE. Rubber Chem Technol 1971;44:440–78.
[24] Lin Q, Gourdon D, Sun C, Holten-Andersen N, Anderson TH, Waite JH, et al. Proc Natl Acad Sci USA 2007;104:3782–6.